European Commission
Research Programme of the Research Fund for Coal and Steel

ANGELHY

Innovative solutions for design and strengthening of telecommunications and transmission lattice towers using large angles from high strength steel and hybrid techniques of angles with FRP strips

WORK PACKAGE 3 – DELIVERABLE 3.4

Development of design rules for closely spaced built-up angle sections

Coordinator:

National Technical University of Athens - NTUA, Greece

Beneficiaries:

ArcelorMittal Belval & Differdange SA - AMBD, Luxembourg

Université de Liege - ULG, Belgium

COSMOTE Kinites Tilepikoinonies AE - COSMOTE, Greece

Centre Technique Industriel de la Construction Métallique - CTICM, France

SIKA France SAS - SIKA, France

Grant Agreement Number: 753993

15/12/2020

AUTHORS:

CTICM
Steel Construction Research Division
Espace Technologique – Immeuble Apollo
L'Orme des Merisiers – F-91193 Saint Aubin
Authors: André Beyer, Guillaume Delacourt, Alain Bureau

Development of design rules for closely spaced built-up angle sections

TABLE OF CONTENTS

1 Introduction

In the framework of Work package WP3 of the project ANGELHY, three configurations of closely spaced built-up members fabricated from angle sections have been studied experimentally and numerically. These different configurations are recalled hereafter:

1) **Back-to-back connected angles** (noted as BBE – see Figure 1.1a)
2) **Star battened angles with equal sections** (noted as SBE – see Figure 1.1b)
3) **Star battened angles with unequal sections** (noted as SBU – see Figure 1.1c)

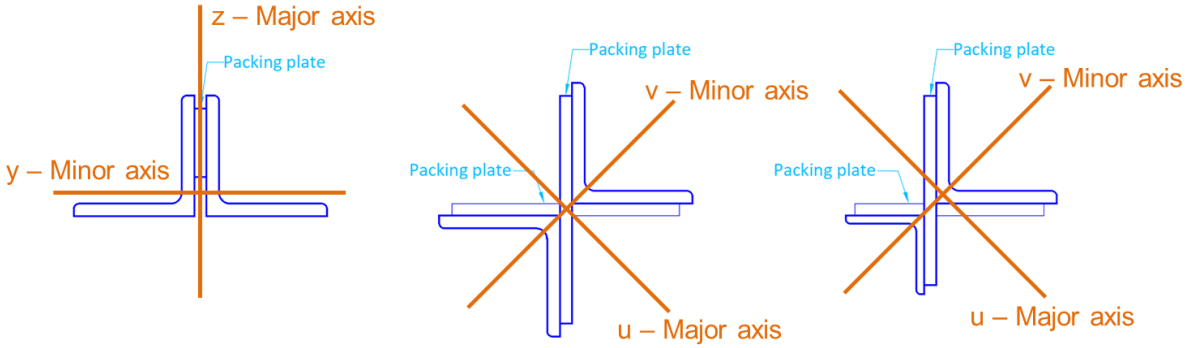

a) BBE **b) SBE** **c) SBU**

Figure 1.1: Typology of closely spaced built-up members

Based on the numerical studies, presented in deliverable D3.3 and the laboratory tests presented in deliverable D3.2, design models are derived hereafter for the three configurations. First, paragraph 2 presents existing design formats and the theoretical basis of the design approach common to all configurations. Then, paragraphs 3.2 and 3.3 present specific design steps to be applied respectively to BBE, SBE and SBU configurations.

2 Existing design procedures

2.1 Theoretical derivations

First, the theoretical derivations presented by Timoshenko and Gere [1] are recalled hereafter. This appears important as most of the design procedures in current standards are based on these developments.

To start up, it is recalled that Engesser has shown that the critical axial force of a column, considering the effect of shearing displacements, can be expressed by Eq. 2.1 [2]:

$$P_{cr} = \frac{P_{cr,1}}{1 + \frac{P_{cr,1} n}{A_v G}} \qquad \textbf{Eq. 2.1}$$

Where: A_v: shear area of the member

G: shear modulus

n: cross-section shape depending constant

In the following, the shear stiffness, expressed by $A_v G/n$ in Eq. 2.1, will be referred to as S_v according to Eurocode 3 notation.

In order to derive an analytical model for the buckling of built-up members, Timoshenko started from the model of a battened column as shown in Figure 2.1. To determine the shear stiffness of the battened column, it is supposed that the bending moment in the chords is 0 at mid-height between two battens. The lateral displacement is determined as sum of the displacements caused by bending of the battens (noted δ_1 – shown in blue on Figure 2.1) and by bending of the chords (noted δ_2 – shown in orange on Figure 2.1).

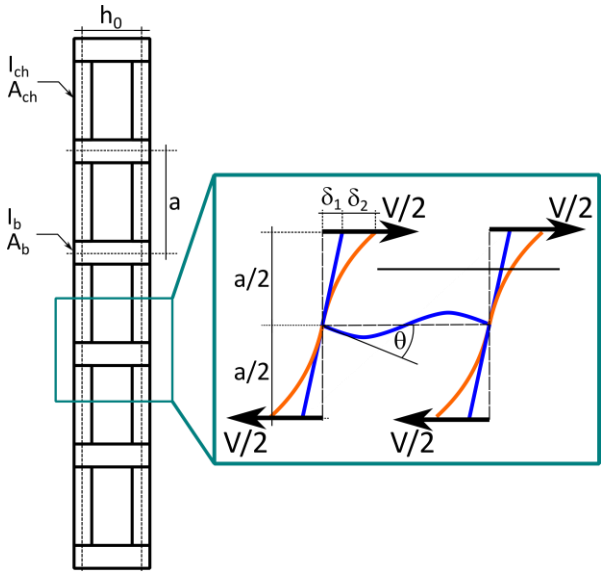

Figure 2.1 Battened column

The angle of rotation at each end of batten can be determined by Eq. 2.2 [1]:

$$\boldsymbol{\theta = \frac{Vah_0}{12EI_b}} \qquad \textbf{Eq. 2.2}$$

Consequently, the lateral displacement δ_1 equals:

$$\boldsymbol{\delta_1 = \frac{Va^2h_0}{24EI_b}} \qquad \textbf{Eq. 2.3}$$

Due to symmetry, the chord behaves as a cantilever beam and consequently, the displacement is obtained by:

$$\boldsymbol{\delta_2 = \frac{Va^3}{48EI_{ch}}} \qquad \textbf{Eq. 2.4}$$

The shear stiffness S_v is defined according to Eq. 2.4 and Figure 2.2.

$$\boldsymbol{\gamma = \frac{V}{S_v}} \qquad \textbf{Eq. 2.5}$$

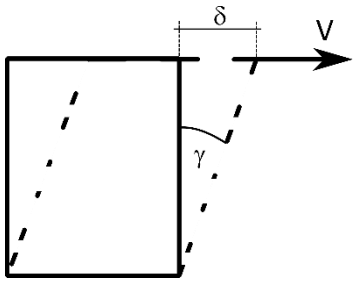

Figure 2.2 Shear displacement

From Figure 2.1, it can be seen that the slope γ is equal to:

$$\boldsymbol{\gamma = \frac{\delta_1 + \delta_2}{a/2}} \qquad \textbf{Eq. 2.6}$$

With Eqs. 2.6, 2.3 and 2.4, it is finally possible to obtain an expression of the shear stiffness of the battened column:

$$\boldsymbol{S_v = \frac{1}{\frac{ah_0}{12EI_b} + \frac{a^2}{24EI_{ch}}}} \qquad \textbf{Eq. 2.7}$$

Eq. 2.7 shows that the shear stiffness depends on the flexural stiffness of the batten and the flexural stiffness of the column. As both, the batten and the chords, are also subjected to shearing forces, the displacement δ may even be greater than $\delta_1 + \delta_2$. An extension of Eq. 2.8 considering the effect of shear stiffness can be found in references [1] and [3]:

$$S_v = \frac{1}{\frac{ah_0}{12EI_b} + \frac{a^2}{24EI_{ch}} + \frac{a}{h_0 GA_{v,b}} + \frac{1}{2GA_{v,ch}}} \qquad \textbf{Eq. 2.8}$$

Where: G: is the shear modulus
$A_{v,b}$: is the shear area of the battens
$A_{v,ch}$: is the shear area of the chord

Finally, in some cases, the connection between battens and chords cannot be considered as concentrated in one single point (as has been done before) but the dimensions of the battens and chords should be considered in the derivation of the shear stiffness. To do so, Snijder derived the following equation [3]:

$$S_v = \frac{1}{\frac{a(h_0 - r_{ch})^3}{12h_0^2 EI_b} + \frac{(a-r_b)^3}{24aEI_{ch}} + \frac{a(h_0 - r_{ch})}{h_0^2 GA_{v,b}} + \frac{(a-r_b)}{2GA_{v,ch}}} \qquad \textbf{Eq. 2.9}$$

Where: r_b: is the height of the batten
r_{ch}: is the height of the chord

Based on the shear stiffness S_v, the critical axial load of a compressed built-up member can be obtained with Eq. 2.10.

$$P_{cr} = \frac{P_{cr,1}}{1 + \frac{P_{cr,1}}{S_v}} = \frac{1}{\frac{1}{P_{cr,1}} + \frac{1}{S_v}} \qquad \textbf{Eq. 2.10}$$

With:

$$P_{cr,1} = EI_{col}\frac{\pi^2}{L^2}$$

$$I_{col} = 2I_{ch} + 0,5A_{ch}h_0^2$$

It should however be noted that the chords themselves may be sensitive to elastic instability if the distance *a* between the battens is high. The critical axial force linked to elastic buckling of the two chords between the battens is given in Eq. 2.11 assuming that the chords are hinged between the battens:

$$P_{cr,ch} = 2EI_{ch}\frac{\pi^2}{a^2} \qquad \textbf{Eq. 2.11}$$

The bending displacement of the chords is increased due to the effect of elastic buckling of the chords between the battens. Consequently, displacement δ_2 of Figure 2.1 becomes:

$$\delta_2 = \frac{Va^3}{48EI_{ch}} \frac{1}{1 - \frac{P_{cr}}{P_{cr,ch}}} \qquad \textbf{Eq. 2.12}$$

Eq. 2.12 supposes that the battened column is subjected to the axial force P_{cr}, which is true at state of elastic instability. With Eq. 2.12 a more refined expression of the critical axial force $\underline{P}_{cr}$ can be obtained (see reference [1]).

$$P_{cr} = \frac{1}{\frac{1}{P_{cr,1}} + \left(\frac{a(h_0 - r_{ch})^3}{12h_0^2 EI_b} + \frac{(a - r_b)^3}{24aEI_{ch}} \frac{1}{1 - \frac{P_{cr}}{P_{cr,ch}}} + \frac{(h_0 - r_{ch})}{h_0^2 GA_{v,b}} + \frac{(a - r_b)}{2GA_{v,ch}} \right)} \qquad \textbf{Eq. 2.13}$$

One may observe that Eq. 2.13 can only be solved iteratively.

In order to avoid an iterative solution, Eurocode 3 Part 1-1 [4] limits the shear stiffness, calculated according to Eq. 2.7 to the critical axial load of the two chords:

$$S_{V,EN} = \frac{24EI_{ch}}{a^2 \left(1 + \frac{2I_{ch}}{I_b a}\right)} \leq \frac{2\pi^2 EI_{ch}}{a^2} \qquad \textbf{Eq. 2.14}$$

Up to this point, the analytical derivation only concerns elastic buckling. The effects of imperfection and plasticity are accounted for in the design methods proposed in different standards and publications. Different approaches are presented hereafter.

2.2 Design procedures in current standards and literature

Approach developed by Bleich [5]:

Following the theoretical works of Timoshenko and Engesser, Bleich proposed a first modified slenderness approach [5]. Based on Eq. 2.10, it is possible to define an effective 2nd moment of area of the built-up column as shown in Eq. 2.15. It should however be noted that Bleich neglected the contribution of the stiffness of the individual chord in the second moment of area of the built-up column which is therefore noted I_{col}^* ($I_{col}^* = I_{col} - 2I_{ch}$).

$$I_{eff} = \frac{1}{\frac{1}{I_{col}^*} + \frac{\pi^2}{L^2} \frac{E}{S_v}} \qquad \textbf{Eq. 2.15}$$

The geometric slenderness of a column is defined as its length divided by its radius of gyration about the considered buckling axis. Therefore, one may write:

$$\boldsymbol{\lambda^2 = \frac{L^2}{i_{eff}^2} = \frac{L^2}{I_{eff}/A}} \qquad \textbf{Eq. 2.16}$$

Using Eq. 2.15 and Eq. 2.16, one may now write:

$$\boldsymbol{\lambda^2 = L^2 \frac{A}{I_{col}^*} + \pi^2 \frac{E}{S_v}} \qquad \textbf{Eq. 2.17}$$

At this point, Bleich neglected the contribution of the batten stiffness to the shear stiffness S_v and therefore obtained:

$$\boldsymbol{\lambda^2 = L^2 \frac{A}{I_{col}^*} + \pi^2 A \frac{a^2}{24 I_{ch}} = L^2 \frac{A}{I_{col}^*} + \pi^2 A \frac{a^2}{24 I_{ch}}} \qquad \textbf{Eq. 2.18}$$

As the area A equals twice the area of one chord, it is possible to introduce the radius of gyration of a chord. Additionally, Bleich introduced at this step the complete expression of the second moment of area of the built-up member I_{col}. It yields:

$$\boldsymbol{\lambda^2 = \left(\frac{L^2}{i_{col}^2} + \frac{\pi^2}{12}\frac{a^2}{i_{ch}^2}\frac{I_{col}^*}{I_{col}}\right)\left(\frac{I_{col}}{I_{col}^*}\right) = \lambda_z^2 \left(\frac{I_{col}}{I_{col}^*}\right) + \frac{\pi^2}{12}\lambda_{ch}^2} \qquad \textbf{Eq. 2.19}$$

As Bleich considered widely spaced built-up columns, the ratio between I_{col} and I_{col}^* is close to 1,0. Consequently, Bleich finally proposed the modified slenderness according to Eq. 2.20.

$$\boldsymbol{\lambda_{zi} = \sqrt{\left(\lambda_z^2 + \frac{\pi^2}{12}\lambda_{z,ch}^2\right)}} \qquad \textbf{Eq. 2.20}$$

Approach developed by Aslani and Goel [6]:

Eq. 2.19 has also been used by Aslani and Goel [6]. However, they considered only the second factor I_{col}/I_{col}^* equal to 1,0. Consequently, they obtain Eqs. 2.21 and 2.22:

$$\lambda_{zi}^2 = \left(\lambda_z^2 + \frac{\pi^2}{12}\frac{I_{col}^*}{I_{col}}\lambda_{zc}^2\right) \quad \textbf{Eq. 2.21}$$

$$\lambda_{zi} = \sqrt{\left(\lambda_z + 0,82\frac{\alpha^2}{1+\alpha^2}\lambda_{zc}^2\right)} \quad \textbf{Eq. 2.22}$$

With:

$$\frac{I_{col}^*}{I_{col}} = \frac{\alpha^2}{1+\alpha^2}$$

$$\alpha = \frac{h_0}{2i_{ch}}$$

One may note that Eq. 2.22 was part of the American standard ANSI/AISC 360-05 [7] and it was applicable for closely spaced built-up members connected through welded connectors or connectors with preloaded bolts. For snug-tight bolts ANSI/AISC 360-05 [7] proposed Eq. 2.23 in which the effect of the chord slenderness is not reduced by any factor.

$$\lambda_{zi} = \sqrt{\lambda_z^2 + \lambda_{z,ch}^2} \quad \textbf{Eq. 2.23}$$

It should be noted that, inversely to the theoretical approaches considering i_{ch} equal to the radius of gyration of the chord about the buckling axis of the built-up column, i_{ch} used to determine the slenderness $\lambda_{z,ch}$ in Eqs. 2.22 and 2.23 is set equal to the minimum radius of gyration of the chord. This can be explained by the fact that the theoretical derivations considered built-up columns mainly made from channel sections whose weak axis is oriented parallel to the buckling axis of the built-up member. In case of back-to-back connected angle sections, this is obviously not the case anymore.

Approach developed by Sato and Uang [8]:

In the 2010 version of ANSI/AISC 360 [9], the equation for built-up sections with welded connectors and connectors with preloaded bolts has been simplified based on the work of Sato and Uang [8]. For back-to-back connected angle sections ANSI/AISC 360-10 proposes:

If $\lambda_1 \leq 40$ then $\lambda_{zi} = \lambda_z$ **Eq. 2.24**

If $\lambda_1 > 40$ then $\lambda_{zi} = \sqrt{\lambda_z^2 + 0,25\lambda_{z,ch}^2}$ **Eq. 2.25**

And $\lambda_1 \leq 0,75\lambda_z$

Owing to the mono-symmetric shape of the back-to-back connected angle sections, the critical axial force for flexural torsional buckling is less than the critical axial force for flexural buckling about the z axis. Therefore, ANSI/AISC 360-10 [9] proposes to calculate the reduction factor according to the following equations:

$$\chi_{ftb} = \begin{cases} 0,658^{\frac{F_y}{F_{e,ftb}}} \; if \; \dfrac{F_y}{F_{e,ftb}} \leq 2.25 \\ 0.877 F_{e,ftb} \; if \; \dfrac{F_y}{F_{e,ftb}} > 2.25 \end{cases} \qquad \textbf{Eq. 2.26}$$

With:

$$H = 1 - \frac{z_s^2}{i_p^2} \qquad \textbf{Eq. 2.27}$$

$$i_p^2 = z_s^2 + \frac{I_y + I_z}{A} \qquad \textbf{Eq. 2.28}$$

Where: z_s: is the position of the shear centre with respect to the centroid, measured along z-axis

I_y/I_z: are the second moment of area about the y-axis/z-axis of the built-up section

A: is the gross area of the built-up section

And:

$$F_{e,fb} = \frac{\pi^2 E}{{\lambda_{zi}}^2} \qquad \textbf{Eq. 2.29}$$

$$F_{e,tb} = \frac{G I_t}{A {i_p}^2} \qquad \textbf{Eq. 2.30}$$

$$F_{e,ftb} = \left(\frac{F_{e,fb} + F_{e,tb}}{2H}\right)\left[1 - \sqrt{1 - \frac{4 F_{e,fb} * F_{e,tb} * H}{\left(F_{e,fb} + F_{e,tb}\right)^2}}\right] \qquad \textbf{Eq. 2.31}$$

ECCS publication n°39 [10] and EN 50341-1 [11]:

As the previous approaches, EN 50341-1 [11] proposes a modified slenderness concept based on ECCS publication n°39 [10] to account for the shear stiffness of the built-up member:

$$\lambda_{zi} = \sqrt{\lambda_z^2 + \lambda_1^2 \frac{m}{2}} \qquad \textbf{Eq. 2.32}$$

Where: λ_z: geometric slenderness of the built-up member considered as uniform - $\lambda_z = L/i_z$

λ_1: geometric slenderness of an individual angle section between packing plates - $\lambda_1 = a/i_v$

m: number of angle sections

As built-up members in the field of lattice towers may be made of 2 or 4 single sections, the number of individual chords enters Eq. 2.32. One may also observe that Eq. 2.32 appears to consider that the connectors are relatively flexible, as the reduction factors included in other modified slenderness approaches are not accounted for. Finally, it is interesting to note that EN 50341-1 does not account for the effect of flexural torsional buckling but only refers to flexural buckling. The applicable reduction factor χ should be determined with buckling curve a_0, which is the most favourable curve of the European buckling curves.

Eurocode 3 Part 1-1 [4]:

Finally, Eurocode 3 Part 1-1 [4] proposes to neglect the effect of the shear stiffness for closely spaced built-up sections for which the packing plate spacing is less than 15 i_{ch} (noted i_{min} in reference [4]). In case of pairs of batten plates (for star battened members), including 2 bolts per packing plate, the distance is increased to 70 i_{ch}. If these distances are not respected, the shear stiffness should be accounted for but Eurocode 3 Part 1-1 does not provide any method explicitly to do so. In reference [12], a simplified and safe-sided method is proposed based on the approach given in Eurocode 3 Part 1-1 for widely spaced built-up columns. Depending on the number of packing plates and the steel grades, reference [12] provides expressions for a modified relative slenderness for back-to-back connected angle sections as shown in Table 2.1. Based on these expressions and buckling curve *b*, the reduction factor for flexural buckling should then be determined. The effect of flexural-torsional buckling is not accounted for.

Table 2.1 Simplified expressions for modified relative slenderness according to reference [12]

Number of packing plates	Steel grade S235	Steel grade S355
2	$\bar{\lambda}_{zi} = 0{,}18\bar{\lambda}_z^2 + 0{,}77\bar{\lambda}_z + 0{,}39$	$\bar{\lambda}_{zi} = 0{,}86\bar{\lambda}_z^2 - 0{,}18\bar{\lambda}_z + 0{,}66$
3	$\bar{\lambda}_{zi} = 0{,}32\bar{\lambda}_z^2 + 0{,}52\bar{\lambda}_z + 0{,}41$	$\bar{\lambda}_{zi} = 0{,}66\bar{\lambda}_z^2 - 0{,}16\bar{\lambda}_z + 0{,}66$
4	$\bar{\lambda}_{zi} = 0{,}56\bar{\lambda}_z^2 + 0{,}17\bar{\lambda}_z + 0{,}48$	$\bar{\lambda}_{zi} = 0{,}65\bar{\lambda}_z^2 - 0{,}21\bar{\lambda}_z + 0{,}67$
5	$\bar{\lambda}_{zi} = 0{,}69\bar{\lambda}_z^2 - 0{,}05\bar{\lambda}_z + 0{,}53$	$\bar{\lambda}_{zi} = 0{,}69\bar{\lambda}_z^2 - 0{,}31\bar{\lambda}_z + 0{,}70$

2.3 Comparison of design approaches

In the following the existing design approaches are compared with each other. To compare the models described above, it is chosen to study the impact of the following criteria:

- The value of yield strength,
- The ratio a/i_{min} that is directly linked to the shear stiffness,
- The number of packing plates.

The field of application of the following comparisons is limited to the field of application of the simplified Eurocode based design approach of reference [12]:

- $15 \leq \frac{a}{i_{min}} \leq 50$
- $t_{angle} = \frac{b}{10} = \frac{h}{10}$
- $50\ mm \leq h = b \leq 200\ mm$
- $2 \leq N \leq 5$
- $f_y = 235\ MPa\ or\ 355\ MPa$
- The thickness of the packing plates is equal to the thickness of the angle section

For the following comparisons, cross section L70x70x7 is considered as chord and the chords are connected back-to-back. The curves are represented with reference to the slenderness noted $\lambda_{z,column}$ referring to the slenderness calculated for the built-up member considered as an homogeneous member without accounting for the possible influence of the connections. This is necessary, as the slenderness modifications are different for the different design approaches. Consequently, the same member would possess a different slenderness for the same length.

Figure 2.3 and Figure 2.4 represent the comparisons based on two different assumptions. First, in Figure 2.3, the results are presented for members possessing the same number of packing plates (3 in the top, 4 in the middle and 5 at the bottom). Consequently, the packing plate distance varies along the curves. In Figure 2.4, the reduction curves are determined based on the same packing plate distance ($15i_{min}$ in the top, $30i_{min}$ in the middle and $50i_{min}$ at the bottom) and therefore the number of packing plates varies along the curve.

Nonetheless, observing the two Figures, the conclusions are the same:

1) The proposal of reference [12] (noted EC – simplified expression) is always most safe-sided;
2) EN 50341-1 yields the most favourable results in all cases;
3) The proposal of Sato and Uang (considered in the 2010 version of ANSI/AISC 360 [9]) leads to results that are conservative for low values of the relative slenderness and become equal to the results obtained with EN 50341-1 for higher values of the relative slenderness;
4) The methods proposed by Bleich and Aslani and Goel practically lead to the same results and correspond to intermediate resistances between the simplified method of reference [12] and the method of EN 50341-1;
5) Both simplified method of reference [12] and the proposal of Sato and Uang do not tend to unity for small values of the relative slenderness.

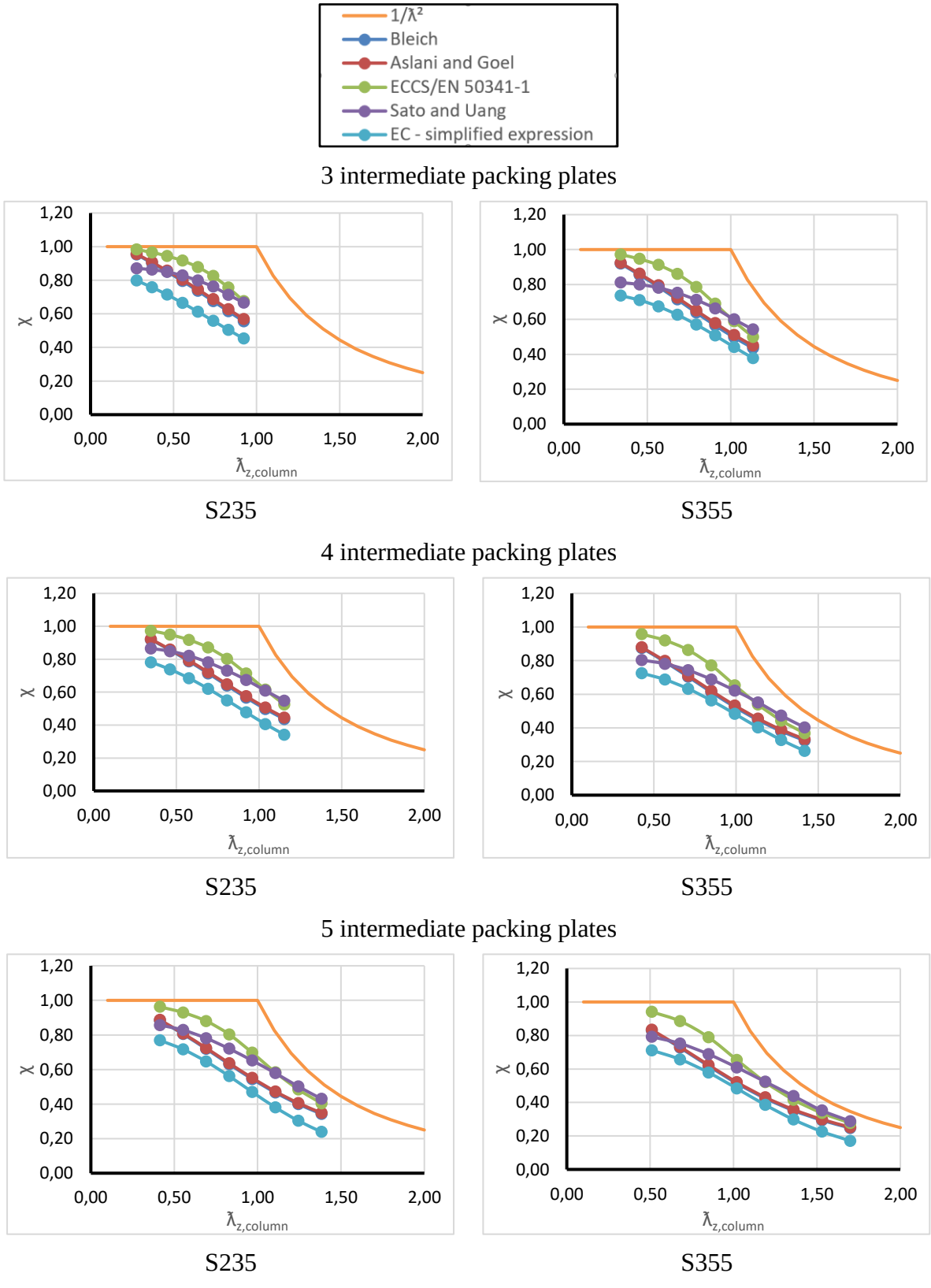

Figure 2.3: Comparison between different design approaches – fixed number of packing plates

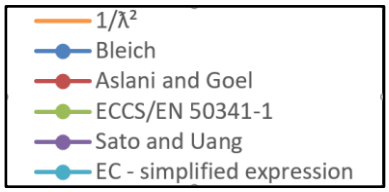

Packing plate distance: $15i_{min}$

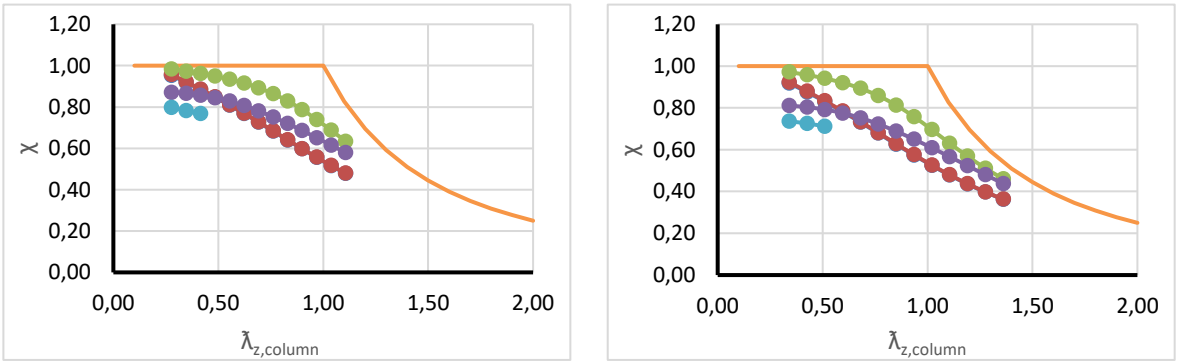

S235 S355

Packing plate distance: $30i_{min}$

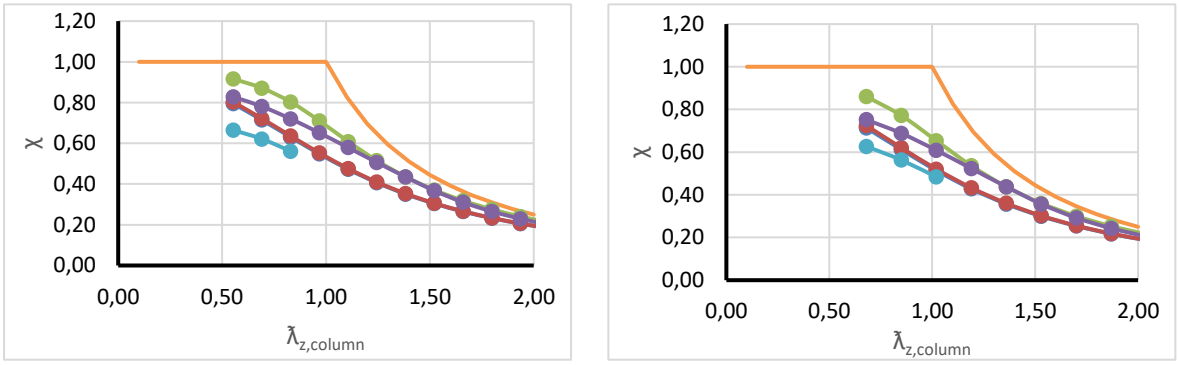

S235 S355

Packing plate distance: $50i_{min}$

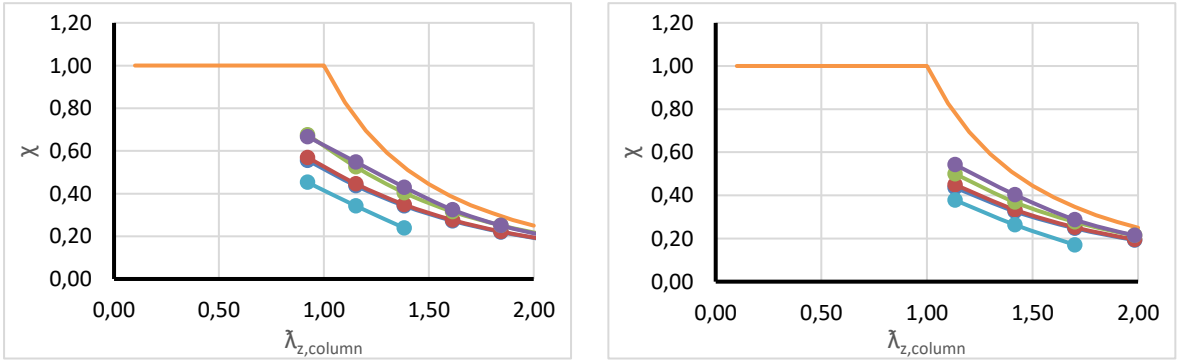

S235 S355

Figure 2.4: Comparison between different design approaches – fixed packing plate distance

Some of the observations may seem surprising at first sight, but they can be explained easily. It is somewhat surprising that EN 50341-1 leads to the most favourable results even if the term linked to the chord slenderness calculated between packing plates is not reduced as for most other design approaches. However, as EN 50341-1 refers to the most favourable buckling curve a_0, the design model becomes very economic.

The simplified method based on Eurocode 3 principles does not tend to unity for small values of the relative slenderness due to the constant summand in the slenderness modification equation (see Table 2.1)

As the simplified method of Eurocode 3, the proposal of Sato and Uang as given in the 2010 version of ANSI/AISC 360 [9] does not lead to unity neither. However, in this case the observation is due to the fact that the failure mode of torsional flexural buckling is accounted for. For short members, the torsional buckling mode becomes more and more predominant compared to the major axis buckling mode (still both are coupled). Additionally, as the warping stiffness is low for angle sections and the built-up members, the critical axial force does not (or only very few) depend on the member length. The ANSI/AISC 360 [9] method therefore tends to a minimum resistance that is independent of the member length.

Finally, as Aslani and Goel modified very few Bleich's method, it seems understandable that both methods lead to very similar resistances.

In order to quantify the observed discrepancies, Table 2.2 summarizes the differences between the design methods relative to the simplified expressions of reference [12]. It is obvious that the differences are very high and consequently a rigorous study of the buckling resistance of closely spaced built-up members is necessary. This study is presented in section 3.2 for BBE specimens and section 3.3 for SBE and SBU specimens.

Table 2.2 Comparison of reduction factor values for the different models

	Bleich	Aslani and Goel	ECCS/EN 50341-1	Sato and Uang	EC Simplified expression [12]
$\lambda_{z,column}$	χ				
0,3	0,92 (+21%	0,92 (+22%)	0,97 (+28%)	0,84 (+10%)	0,76
0,5	0,84 (+18%)	0,84 (+18%)	0,95 (+33%)	0,82 (+15%)	0,71
1,0	0,52 (+8%)	0,53 (+10%)	0,67 (39%)	0,62 (+27%)	0,48
1,5	0,29 (+30%)	0,30 (+32%)	0,34 (+49%)	0,35 (+56%)	0,23
2,0	0,19	0,19	0,22	0,21	-

3 Design approach proposed for closely-spaced built-up members

3.1 General

The design approaches are derived and validated based on the numerical model presented in detail in Deliverable 3.3 of the ANGELHY project. Hereafter, only the general features of this model are recalled. The numerical results are based on simulations accounting for:

- Geometric non linearities (including contact non linearity and 2nd order effects);
- An elastic perfectly plastic material law according to Figure 3.1;
- The residual stress pattern according to Figure 3.2;
- A geometric imperfection with an amplitude of L/1000. For BBE specimens the imperfection is chosen affine to a sine half wave about the major axis (failure mode of major axis buckling is studied) and for SBE and SBU specimens the imperfection is chosen equal to a sine half wave about the minor or major axis depending on the studied failure mode.

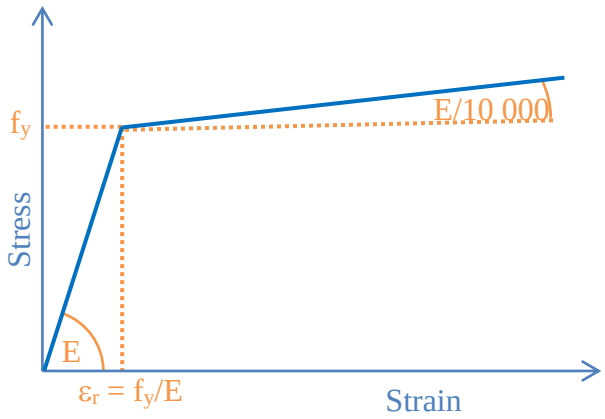

Figure 3.1: Bi-linear stress-strain curved used for preliminary study of the laboratory tests

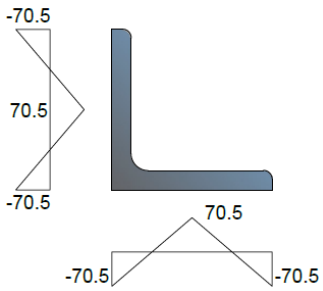

Figure 3.2: Residual stress model

3.2 Design model for major axis buckling of back-to-back connected members

Throughout this paragraph, the development of the design model for major axis buckling (about z-axis – see Figure 1.1) of back-to-back connected members is presented. The minor axis

buckling does not mobilize the connection stiffness and may therefore be treated with the design model for buckling of individual angle section members developed in Work Package 2 of ANGELHY. Additionally, it may be noted that the torsional flexural buckling mode does not become relevant as this has already been shown for single angle sections. Consequently, only flexural buckling about the major axis is considered in the following.

Figure 3.3, Figure 3.4 and Figure 3.6 show the results obtained for BBE members connected with fitted bolts, preloaded bolts and snug tight bolts. In the framework of this study snug tight bolts are considered without any preloading even if this is very conservative in practice. It is recalled that the sensitivity study presented in Deliverable 3.3 of the ANGELHY project highlighted that:

- A preloading equal to 20% of a nominal full preloading together with a friction coefficient of 0,3 leads to practically the same resistance as a BBE members connected through fully preloaded bolts;
- The number of packing plates does not influence the resistance of built-up members if the connection is realized with snug tight (non-preloaded) bolts.
- The resistance of BBE members connected through snug tight bolts is higher than the sum of buckling resistances of the two individual chords.

In practice, a snug tight connection will always lead to resistances higher than the lower bound presented hereafter as a certain preloading is always applied. Nonetheless, the initial value of this preloading cannot be guaranteed and the loss of preloading with time cannot be quantified. Consequently, the proposal provided hereafter will be based on the lower bound.

The following figures indicate that it is possible to represent the numerically obtained results in form of a λ-χ diagram without a noticeable influence of the packing plate distance (varied between ($15i_{min}$ and $50i_{min}$). Indeed, the effect of the packing plate distance, and consequently the effect of the shear stiffness, is accounted for in the calculation of the relative slenderness according to Equations 3.1 and 3.2.

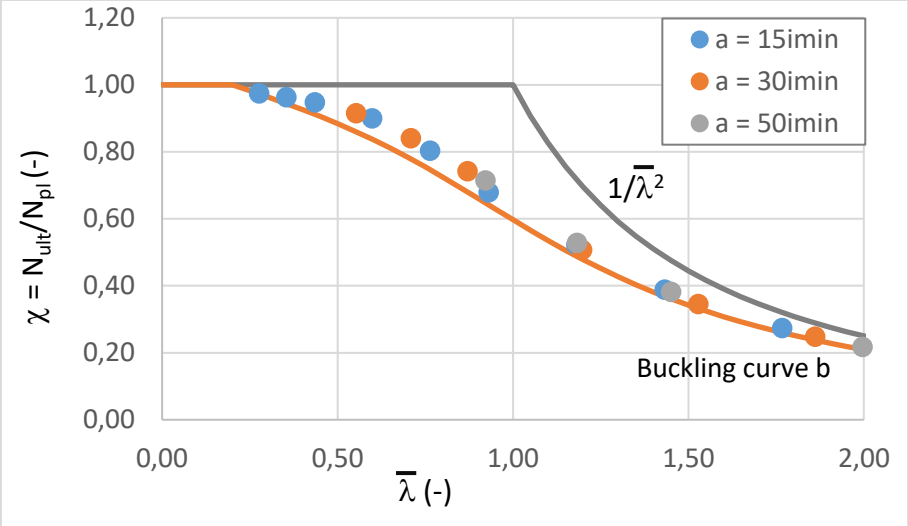

Figure 3.3: Numerical results for BBE specimens with fitted bolts

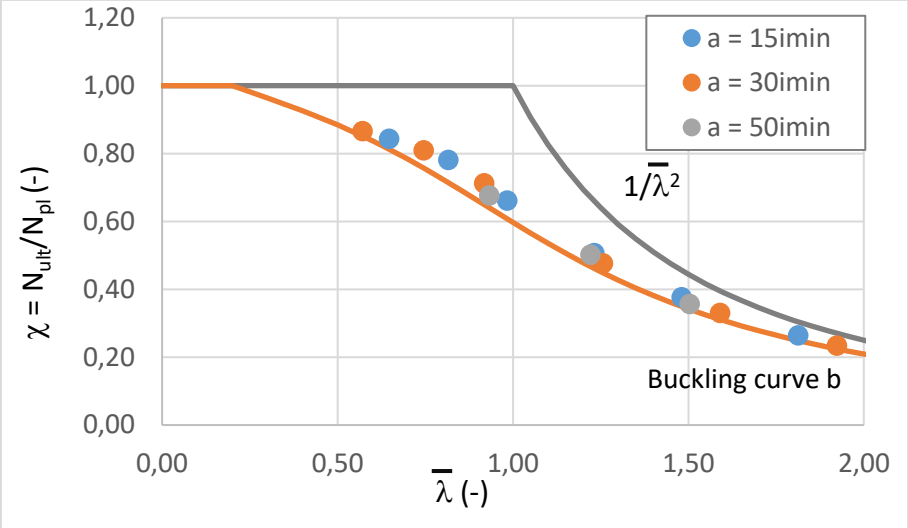

Figure 3.4: Numerical results for BBE specimens with preloaded bolts

$$\bar{\lambda} = \sqrt{\frac{A f_y}{N_{cr,Sv}}} \qquad \textbf{Eq. 3.1}$$

$$N_{cr,Sv} = \frac{1}{\frac{1}{N_{cr,z}} + \frac{1}{S_v}} \qquad \textbf{Eq. 3.2}$$

$$N_{cr,z} = 2EI_z \left(\frac{\pi}{L}\right)^2 \qquad \textbf{Eq. 3.3}$$

Where:

$N_{cr,z}$: is the critical axial force for buckling about the z-axis of the built-up member considered as a homogeneous member (neglecting the effect of the shear stiffness)

E: is the Young's modulus

I_z: is the second moment of area of the built-up member considered as a homogeneous member (neglecting the effect of the shear stiffness)

L: is the length of the member

S_v: is the shear stiffness of the built-up member

In order to determine an appropriate equation of the shear stiffness, the critical axial forces $N_{cr,Sv}$ have been determined through linear buckling analysis performed with the numerical model. The obtained results have then been compared to analytical expressions of $N_{cr,Sv}$. By doing so, it was possible to validate the use of Eqs. 3.4 and 3.5 for fitted bolt connections and preloaded connections, respectively.

Fit bolts:

$$S_v = \frac{1}{\frac{a^2}{24EI_{v,ch}}} e \qquad \textbf{Eq. 3.4}$$

Preloaded bolts:

$$S_v = \frac{1}{\frac{a^2}{24EI_{v,ch}} + \frac{ah_0}{12EI_{pp}}} \qquad \textbf{Eq. 3.5}$$

and:

$$I_{pp} = \frac{\pi(d+2t)^4 - \pi d_0^4}{32} \qquad \textbf{Eq. 3.6}$$

Where:

I_{pp}: is the second moment of area of the packing plate contributing to the shear stiffness

t: is the thickness of the angle section

d: is the diameter of the bolt

d_0: is the diameter of the hole

Eq. 3.6 assumes that the preloading force acting in the bolt spreads in an angle of 45° through the leg of the angle section starting from the bolt head. The comparisons between the critical axial forces obtained analytically and those obtained through numerical simulations (noted $N_{cr,LBA}$) are given in Figure 3.5. One may observe that the analytical formulae leads to globally satisfactory results. Nonetheless, they seem to be slightly conservative. Indeed, in average the ratio $N_{cr,LBA}/N_{cr,analyt}$ is equal to 0,95 for fit bolt and 0,97 for preloaded bolt connections. Obviously, the simplified formulae do not cover all parameters influencing the shear stiffness S_v and consequently the critical axial force. Nonetheless, using the simplified formulae in the design model still leads to very satisfactory and safe-sided results for the buckling resistance.

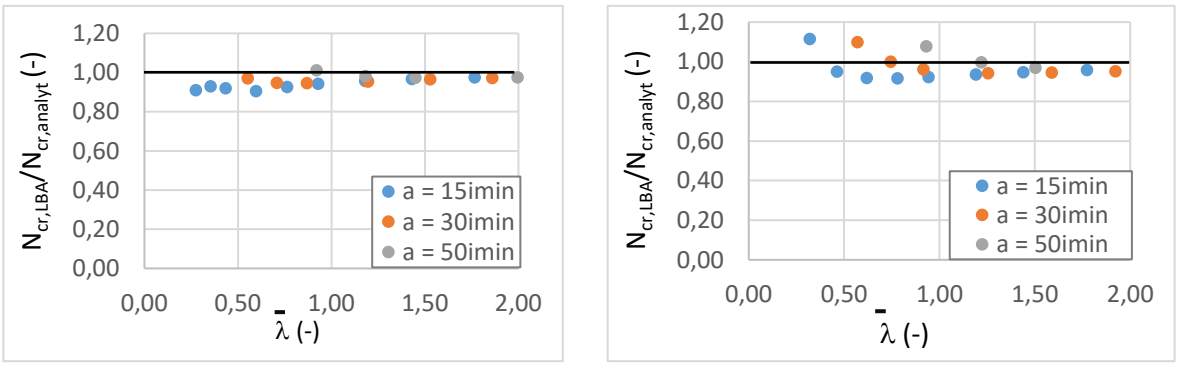

a) Connection with fit bolts b) Connection with preloaded bolts

Figure 3.5: Comparison of numerically and analytically determined critical axial forces

In contrary to connections with fit bolts and preloaded bolts, the number of packing plates (and therefore the packing plate distance) does not have any influence on the major axis buckling resistance. Nonetheless, it should be noted that if the packing plates were omitted, the buckling mode would obviously not be buckling about the major axis of the built-up member but buckling of two individual members about their respective minor axis. Consequently, the packing plates force the built-up member to buckle about its major axis. In order to fulfil this function, a minimum number of two intermediate packing plates is however necessary.

Figure 3.6 shows the numerical simulations in the λ-χ diagram. Again, the numerical simulations are well aligned with buckling curve *b*. The relative slenderness has been obtained based on critical axial force determined with a modified slenderness resulting from the boundary conditions at the ends. In fact, due to the connection of the individual angle sections to the gusset plate at the member ends, a certain rotational stiffness is provided reducing the buckling length to approximatively 0,75L. Consequently, in case of snug tight bolt connections, the critical axial force may be obtained with:

Snug tight bolts:

$$N_{cr,z} = 2EI_{z,ch}\left(\frac{\pi}{0,75L}\right)^2 \qquad \textbf{Eq. 3.7}$$

Where:

$I_{z,ch}$: is the second moment of area of an individual angle section about its z-axis

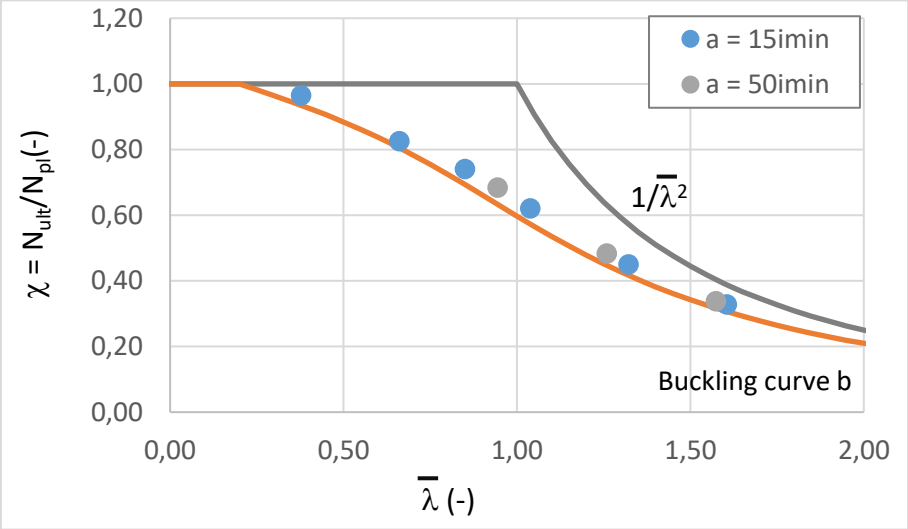

Figure 3.6: Numerical results for BBE specimens with snug tight bolts

Finally, it seems interesting to compare the resistances of the BBE members depending on the connection type. This comparison cannot be done anymore with reference to λ as the value of the relative slenderness depends on the connection type. Consequently, the same member would not have the same relative slenderness if the connections are realised with snug tight bolts or fit bolts. In order to have a meaningful comparison, the member length is therefore used as reference.

In Figure 3.7, one may observe the results of this comparison of built-up members fabricated from L70x70x7. The fit bolt connection leads to the highest resistance. The snug tight bolt connections lead to a strength reduction of about 5 to 15% depending on the member length. The highest difference is obtained for intermediate values of the member length. The preloaded bolt connection leads to intermediate values between the two other cases.

For simplicity, it seems therefore possible to design BBE members independently from the connection type, the lower bound resistance of snug tight bolt connections without being too conservative.

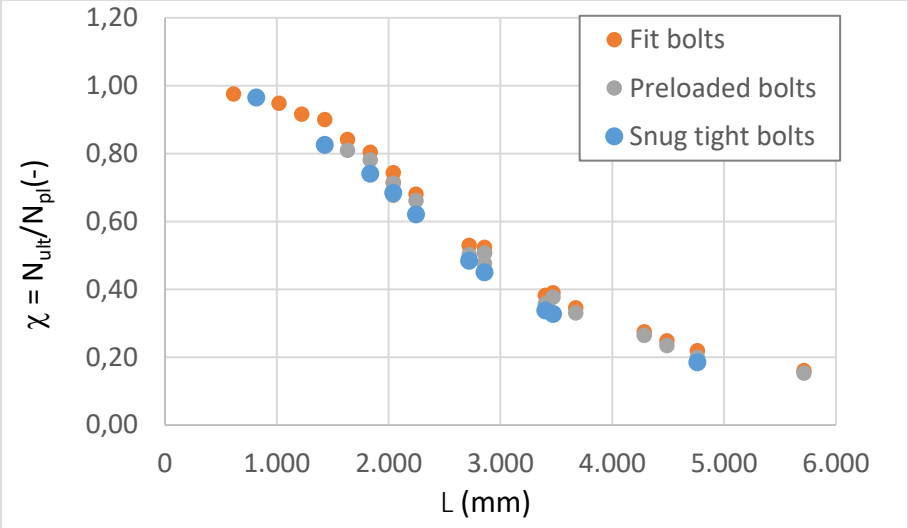

Figure 3.7: Comparison of resistances between different connection types

Up to this point, all members where considered as fabricated from S355. The influence of the yield strength is shown in Figure 3.8, presenting results for fit bolt connections. It seems that increasing the yield strength has also the tendency to increase the buckling resistance. However, based on the numerical results it seems not possible to reliably link buckling curve *a* to built-up members fabricated from S460.

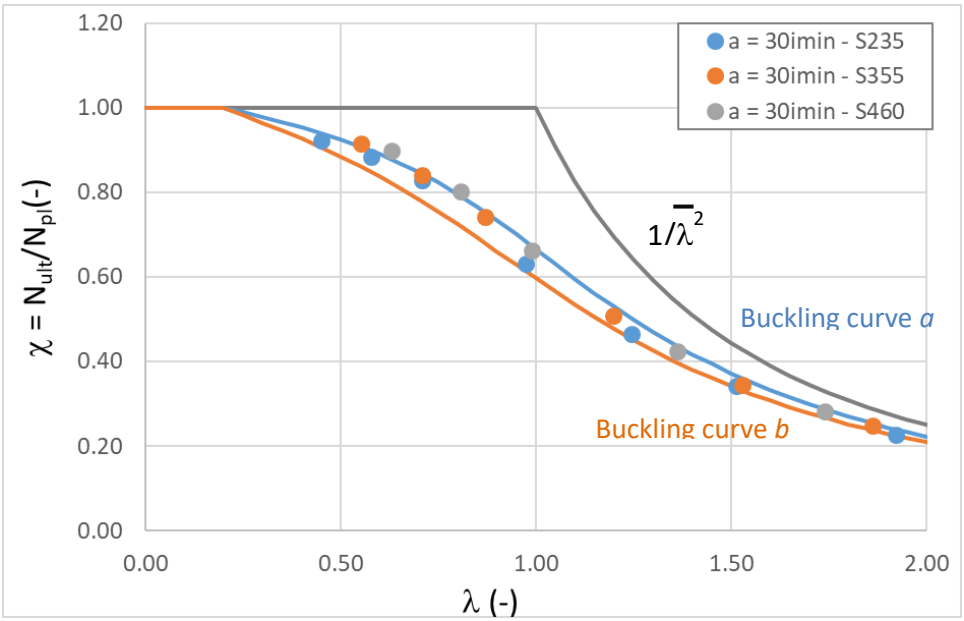

Figure 3.8: BBE buckling resistance depending on the steel grade

3.3 Design model for buckling of star battened built-up member subject to a combination of axial force and bending moments

3.3.1 Format of the chosen design model

The design model proposed for star battened angle section members has been developed, based on the assumption that the angle sections are connected through a pair of batten plates and two times four bolts per connection as schematically shown in Figure 3.9.

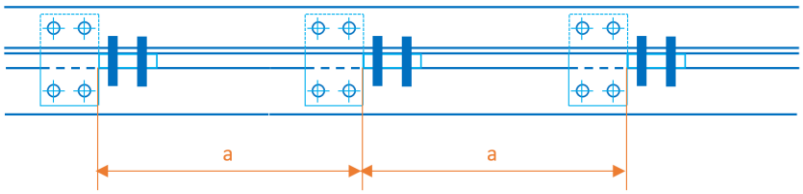

Figure 3.9: Definition of the distance between batten plates

The axis definition for star battened members is recalled in Figure 3.10.

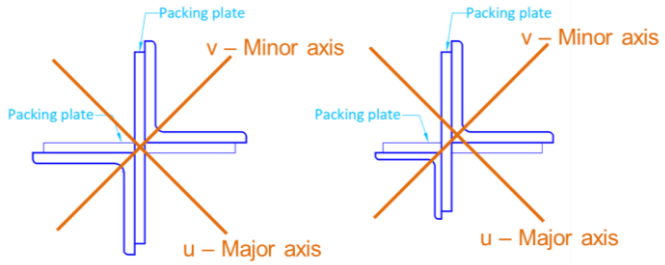

Figure 3.10: Definition of axes for star battened members

In order to propose a uniform set of design equations in the framework of ANGELHY, it has been chosen to use the same format of interaction equations that has been developed for single angle section members in steel and hybrid single angle section members. This format is recalled in Eqs. 3.8 and 3.9.

$$\left(\frac{N_{Ed}}{\chi_u \frac{N_{Rk}}{\gamma_{M1}}} + k_{uu}\frac{M_{u,Ed}}{\chi_{LT}\frac{M_{u,Rk}}{\gamma_{M1}}}\right)^{\xi} + k_{uv}\frac{M_{v,Ed}}{\frac{M_{v,Rk}}{\gamma_{M1}}} \leq 1 \qquad \textbf{Eq. 3.8}$$

$$\left(\frac{N_{Ed}}{\chi_v \frac{N_{Rk}}{\gamma_{M1}}} + k_{vu}\frac{M_{u,Ed}}{\chi_{LT}\frac{M_{u,Rk}}{\gamma_{M1}}}\right)^{\xi} + k_{vv}\frac{M_{v,Ed}}{\frac{M_{v,Rk}}{\gamma_{M1}}} \leq 1 \qquad \textbf{Eq. 3.9}$$

The interaction factors k_{ij} are given in Table 3.1.

Table 3.1: Interaction factors k_{ij}

Interaction factors	$k_{uu} = \frac{C_u}{1 - \frac{N_{Ed}}{N_{cr,u}}}$	$k_{vu} = C_u$
	$k_{uv} = C_v$	$k_{vv} = \frac{C_v}{1 - \frac{N_{Ed}}{N_{cr,v}}}$
Equivalent uniform moment factors	$C_u = 0{,}6+0{,}4\psi_u \geq 0{,}4$ und $-1 \leq \psi_u = \frac{M_{2u}}{M_{1u}} \leq 1$	
	$C_v = 0{,}6+0{,}4\psi_v \geq 0{,}4$ und $-1 \leq \psi_v = \frac{M_{2v}}{M_{1v}} \leq 1$	

In order to adapt the interaction equations to the case of star battened built-up members, it is necessary to calibrate the following particular points:

- The buckling resistance under an axial compression force only;
- The lateral torsional buckling resistance;
- The exponent ξ.

The validity of the interaction factor k_{ij} is not questioned here as they have been derived from elastic second order theory independently from the shape of the cross section.

3.3.2 Resistance of star battened built-up members under compression

Hereafter, only the buckling resistance of SBE and SBU specimens with fit bolts is presented. The influence of the connection type may be accounted for through the determination of a connection specific shear stiffness as for BBE specimens. However, it will be shown in the following that the influence of the shear stiffness on the member resistance is much less than for BBE specimens and that it may be neglected in some well-defined cases.

Figure 3.11 represents the results for minor axis buckling of SBE specimens composed of 2 L70x70x7. The numerical results are again aligned with buckling curve *b*. One may note that the shear stiffness is not accounted for. Only two cases appear to be unsafe compared to buckling curve *b*. These cases are members that possess only one pair of intermediate battens. Therefore, it seems possible to neglect the effect of the shear stiffness if at least two pairs of intermediate packing plates are used up to a distance between the battens equal to $90i_{min}$. Higher, distances are not studied in the framework of ANGELHY as the slenderness of the built-up member becomes too high for practical applications even for the use of a very low number of batten plates.

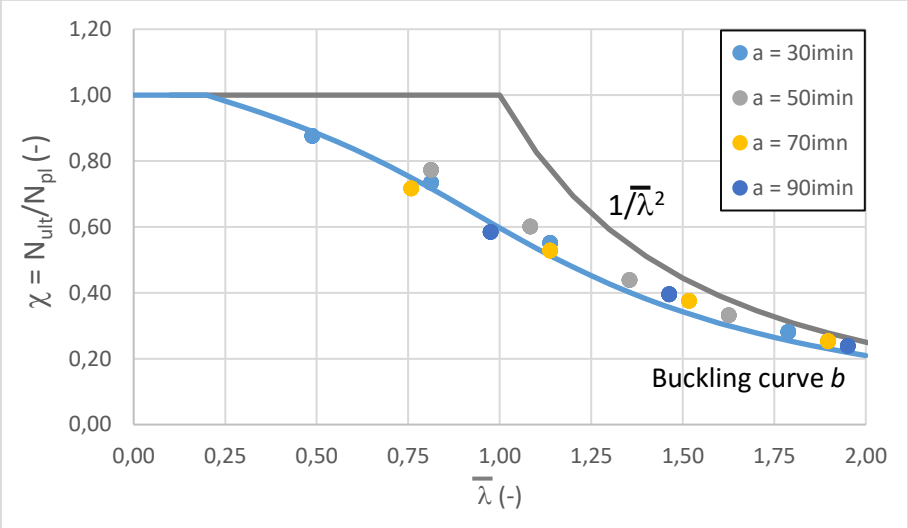

Figure 3.11: Minor axis buckling of SBE specimens – Shear stiffness <u>not accounted</u> for

Next, the minor axis buckling resistance of SBU specimens composed of one L90x90x9 and one L60x60x6 section. The batten thickness is 8 mm and the angle section are connected with fit bolts. Additionally, it should be noted that at least 2 intermediate pairs of battens are used. Figure 3.12 shows again that the effect of the shear stiffness may be neglected up to a distance between battens of $90i_{min}$. In case of SBU specimens this distance has been calculated using the minimum radius of gyration of the smaller angle section.

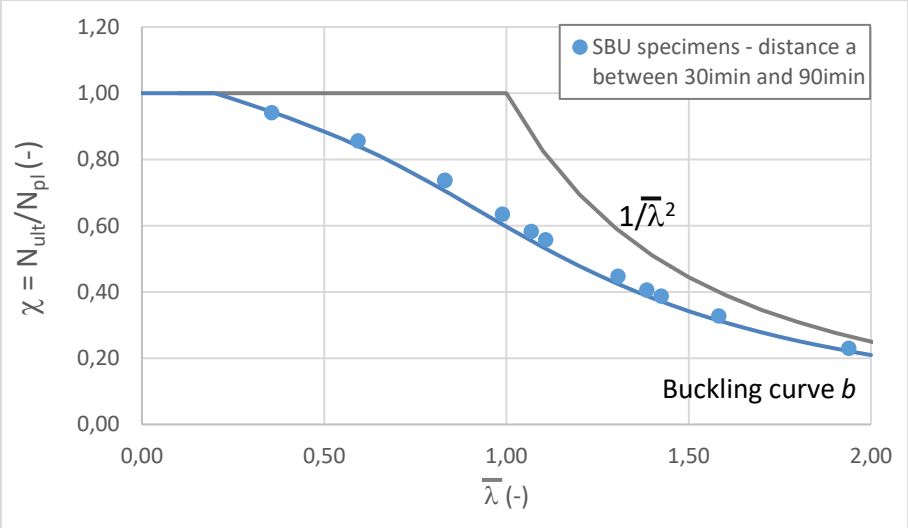

Figure 3.12: Minor axis buckling of SBU specimens – Shear stiffness <u>not accounted</u> for

It should be noted that it is not surprising that the minor axis buckling resistance does not mobilise the shear stiffness of the built-up member as this failure mode corresponds to the buckling of two individual members. In fact, the second moment of area is simply the sum of the second moments of area of the two individual chords.
For major axis buckling, however, the Steiner's contribution is mobilised and consequently the shear stiffness affects the buckling resistance of the member as shown in Figure 3.13 and Figure

3.14. Figure 3.14 shows that the results become unsafe, even only slightly, if the effect of the shear stiffness is neglected. One may note that the shear stiffness has been calculated as shown in Eq. 3.10 with reference to the minor axis second moment of area of the taller section. The minor axis second moment of area is used here, as it is parallel to the major axis of the built-up member.

$$S_v = \frac{1}{\frac{a^2}{24EI_{v,ch,1}}} \qquad \textbf{Eq. 3.10}$$

Where:
$I_{v,ch,1}$: is the second moment of area of the taller angle section about its minor axis

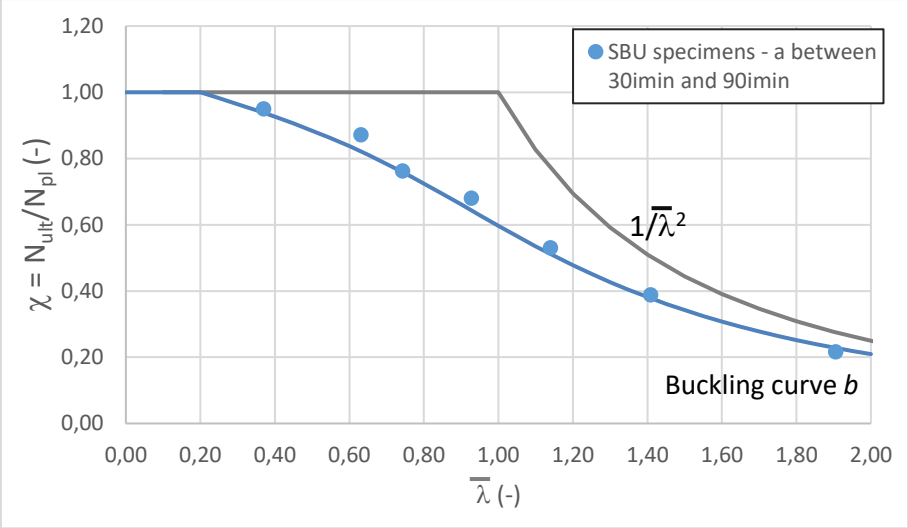

Figure 3.13: Major axis buckling of SBU specimens – Shear stiffness <u>accounted</u> for

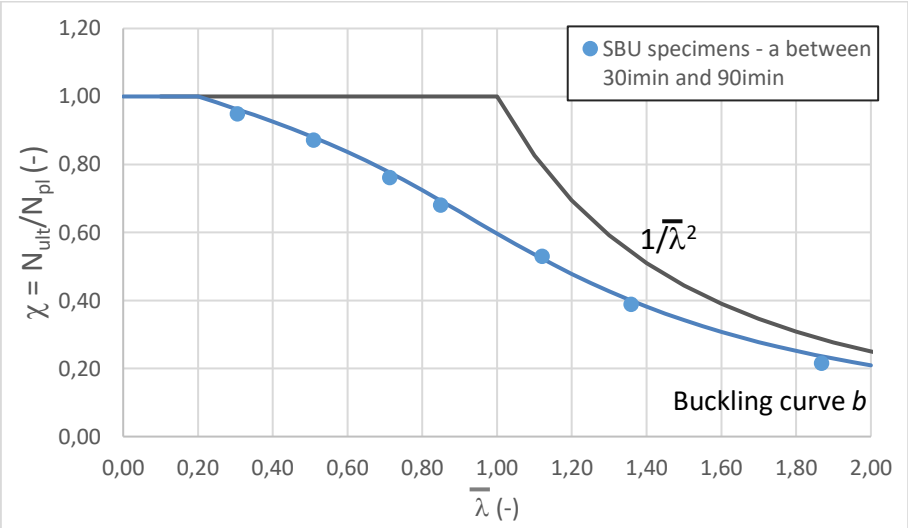

Figure 3.14: Major axis buckling of SBU specimens – Shear stiffness <u>not accounted</u> for

3.3.3 Resistance of star battened built-up members under major axis and minor axis bending

Hereafter, the bending moment resistance of star battened built-up members is highlighted based on the example of a SBE member fabricated from S355 and two L70x70x7 sections. Even though, it is generally accepted that instability only occurs under major axis bending, the members are also studied under the effect of a minor axis bending moment. The bending moments are constant along the members.

The critical bending moment is determined with Eq. 3.11. This equation corresponds to the usual equation also used for double symmetric I sections but it is considered that the warping stiffness vanishes for the star battened members. In case of minor axis bending, the same equation is applied but I_v is replace by I_u. Finally, the relative slenderness is obtained with Eq. 3.12.

$$M_{cr} = C_1 \pi \frac{\sqrt{E I_v G I_t}}{L} \qquad \textbf{Eq. 3.11}$$

$$\bar{\lambda}_{LT} = \sqrt{\frac{M_{pl}}{M_{cr}}} \qquad \textbf{Eq. 3.12}$$

Where:

G: is the shear modulus

I_t: is the torsion constant

Figure 3.15 represents the obtained ultimate resistances. At first, one may observe that even in case of minor axis bending, the ultimate minor axis bending moment is reduced compared to the plastic minor axis bending moment. This astonishing result seems to indicate that lateral torsional buckling may also be relevant if the member is subjected to minor axis bending.

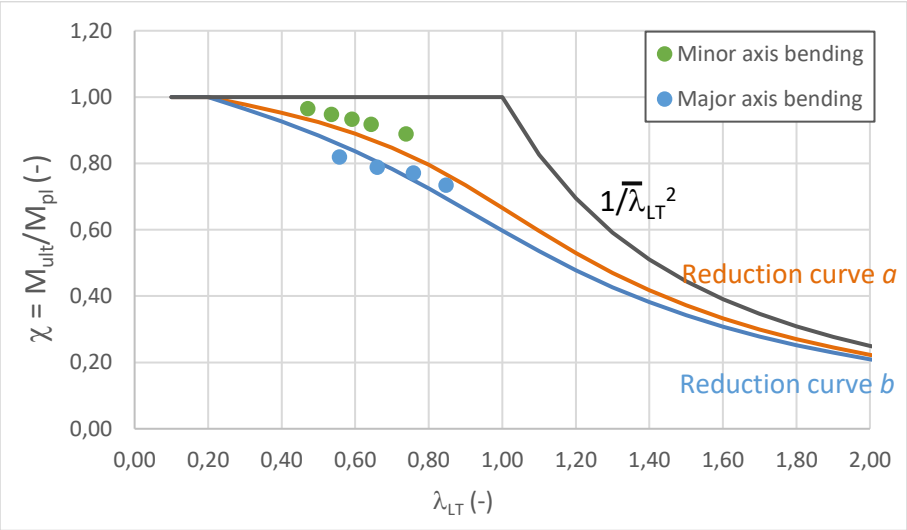

Figure 3.15: Resistance of SBE specimens subject to minor and major axis bending

In order to analyse the results further on, Figure 3.16 represents the displacement vectors at the maximum load level for the SBE member subject to minor axis bending and possessing a relative slenderness of about 0,6. One may observe that the member does not move perpendicularly to the bending axis. Additionally, one may not observe any rotation. Consequently, it seems that instability is not the origin of the strength reduction under minor axis bending. Indeed, the bending moment resistance is reduced due to the presence of the bolt hole at the tensions side.

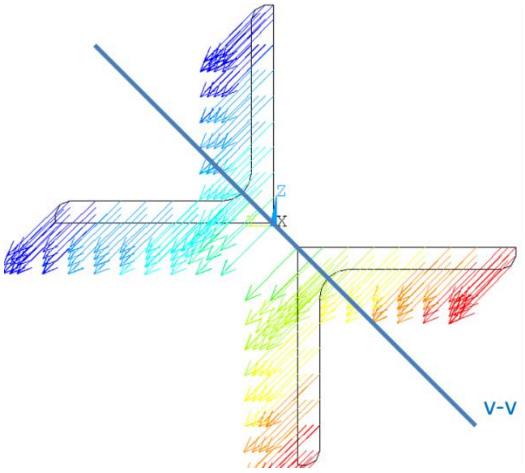

Figure 3.16: Displacement vectors at maximum load for a member subject to minor axis bending – λ_{LT} = 0,60

The results are recalculated again with reference to the reduced bending moment resistance. One may note that the reduction of the bolt hole leads to a reduction of approximatively 10% of the minor and major axis plastic bending moment. In Figure 3.17, the results are presented with reference to the reduced bending moment resistance that has been calculated exactly by reducing the bolt hole from the section. It appears that the built-up members attain this reduced reference resistance. Nonetheless, it seems that increasing the member length leads to a reduction of the minor axis bending moment resistance. Yet, for a relative slenderness of 0,7 under minor axis bending the member length is approximatively equal to 6700 mm. This seems to be at the upper bound of practical interest as this length leads to a relative flexural buckling slenderness of about 2,2. Therefore it seems possible to neglect any length effect and consider the minor axis bending moment resistance equal to $0{,}9M_{pl,v}$.

For members subject to major axis bending, the reduction of the reference resistance also changes the results. If one refers to the reduced bending moment resistance, it seems possible to apply reduction curve *a* to assess the lateral torsional buckling resistance of built-up members subject to major axis bending.

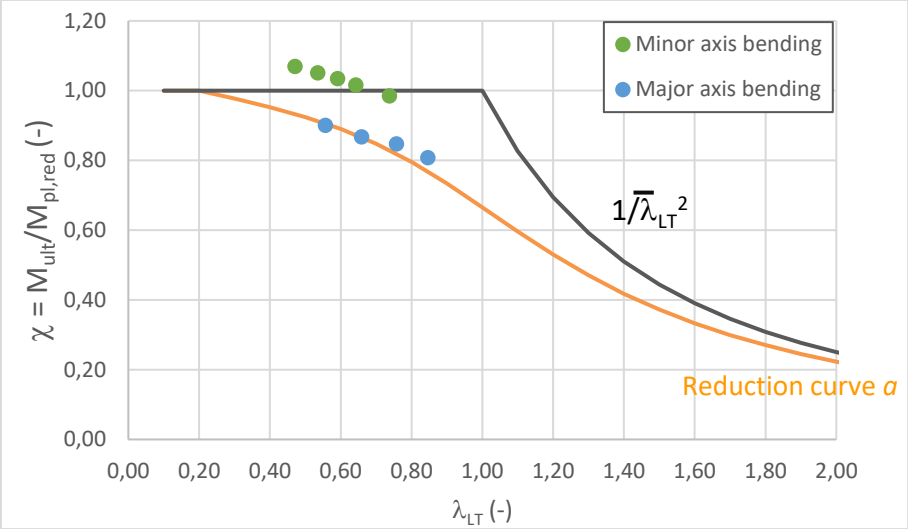

Figure 3.17: Resistance of SBE specimens subject to minor and major axis bending

3.3.4 Resistance of star battened built-up members under combined axial force and bi-axial bending

3.3.4.1 Built-up members subject to minor axis bending and compression

In this section, the members are studied under combined minor axis bending and compression (see Figure 3.10 for the definition of axes). As it has been shown in section 3.3.2, the shear stiffness does not influence the bending stiffness of the built-up member in this case.
In absence of the major axis bending moment, the interaction equations used for design reduce to:

$$\left(\frac{N_{Ed}}{\chi_v \frac{N_{Rk}}{\gamma_{M1}}}\right)^{\xi} + k_{vv}\frac{M_{v,Ed}}{\frac{M_{v,Rk}}{\gamma_{M1}}} \leq 1 \qquad \textbf{Eq. 3.13}$$

$$k_{vv} = \frac{C_v}{1 - \frac{N_{Ed}}{N_{cr,v}}} \qquad \textbf{Eq. 3.14}$$

A maximum value of 2 was chosen for the exponent ξ in case of single angle sections. A preliminary evaluation of the numerical results has shown that this value was too high for built-up members. Therefore, the exponent is reduced to 1,5 for SBE specimens and 1,1 for SBU specimens. It may be noted that only compact sections have been studied in case of built-up members. Consequently, the exponent ξ does not vary. Nevertheless, if semi-compact or slender angle sections are used ξ should probably be reduced but these sections are outside of the scope of the study on built-up members.

Figure 3.18 shows the evaluation of the ratio between the resistance obtained by applying the interaction equation R_{Method} and the resistance obtained through numerical simulations R_{GMNIA}. As an example, the results obtained for SBE sections fabricated from 2L70x70x7 and SBU sections fabricated from L90x90x9 and L60x60x6 are represented in Figure 3.18. The

connections are fabricated with fit bolts. Nonetheless, the shear stiffness of the member does not influence its behaviour.

One may observe that the results are generally safe. Additionally, one may observe that the sum of the mean value and one standard deviation is close to one, which is a first indicator of a satisfactory reliability (see section 3.4 for the calculation of the partial factors).

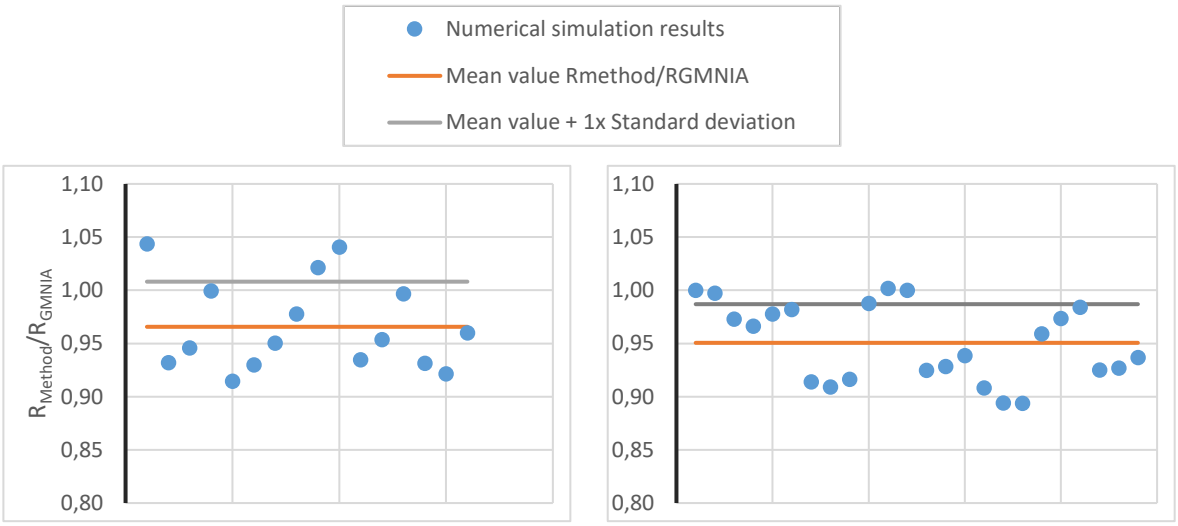

a) SBE specimens **b) SBU specimens**

Figure 3.18: Resistance of SBE specimens subject to minor and major axis bending

3.3.4.2 Built-up members subject to major axis bending and compression

Next, members subject to combined major axis bending and compression (see Figure 3.10 for the definition of axes) are studied. In case of buckling about the major axis, the shear stiffness of the built-up member is mobilized and consequently its effect should be accounted for in the calculation of the critical axial force $N_{cr,u}$. However, for low values of the bending moment, buckling about the minor axis may be relevant. Therefore, two interaction equations should be used in order to assess the resistance of built-up members subject to combined major axis bending and compression.

$$\frac{N_{Ed}}{\chi_u \frac{N_{Rk}}{\gamma_{M1}}} + k_{uu} \frac{M_{u,Ed}}{\chi_{LT} \frac{M_{u,Rk}}{\gamma_{M1}}} \leq 1 \qquad \textbf{Eq. 3.15}$$

$$\frac{N_{Ed}}{\chi_v \frac{N_{Rk}}{\gamma_{M1}}} + k_{vu} \frac{M_{u,Ed}}{\chi_{LT} \frac{M_{u,Rk}}{\gamma_{M1}}} \leq 1 \qquad \textbf{Eq. 3.16}$$

$$k_{uu} = \frac{C_u}{1 - \frac{N_{Ed}}{N_{cr,Sv,u}}}$$

$$k_{vu} = C_v$$

Figure 3.19 represents the ratio between the resistance of the studied members obtained through the application of the interaction equations, noted R_{Method}, and the resistance obtained through numerical simulations, noted R_{GMNIA}. Results are given for SBE members fabricated from 2 L70x70x7 and for SBU members fabricated from L90x90x9 and L60x60x6. It may be observed that all results are safe sided (ratio $R_{Method}/R_{GMNIA} < 1,0$). The Mean value is equal to 0,87 for SBE members and 0,85 for SBU members. It appears therefore that the proposed design equations are more conservative than in case of members subject to an axial compression force and minor axis bending. This additional conservatism may be linked to the format of the interaction equations. In fact, the non-linear plastic interaction on the cross section level is covered, in a simplified way, for the load combination $N+M_v$ by the exponent ξ. In case of the load combination $N+M_u$, the interaction at the cross section level is supposed to be linear. Possible plasticity is only accounted for in the reference resistances N_{Rk} and $M_{u,Rk}$. The interaction factors k_{uu} and k_{vu} have been derived, based on elastic second order theory and do not cover the beneficial effects arising from plasticity. Nonetheless, the observed conservatism is accepted here, as the objective is the development of a practical and easy to apply design approach.

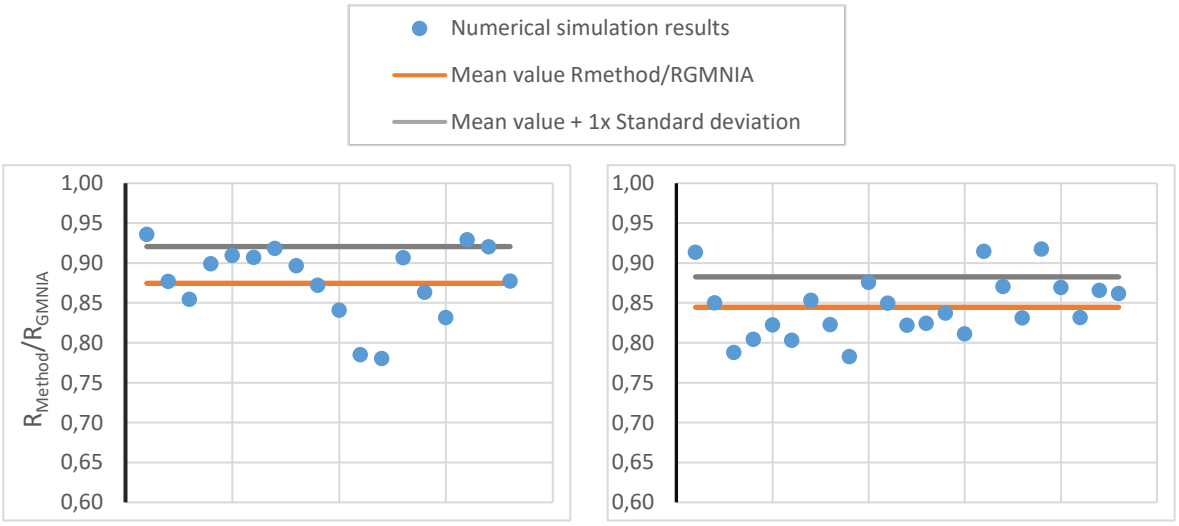

a) SBE specimens **b) SBU specimens**

Figure 3.19: Resistance of SBE and SBU specimens subject to combined axial force and major axis bending

3.3.4.3 Built-up members subject to major axis bending and compression

Finally, section 3.3.4.3 studies the resistance of built-up members subject to axial compression and bi-axial bending. In this case, the complete set of interaction equations recalled in Eqs. 3.17 and 3.18 has to be applied.

$$\left(\frac{N_{Ed}}{\chi_u \frac{N_{Rk}}{\gamma_{M1}}} + k_{uu}\frac{M_{u,Ed}}{\chi_{LT}\frac{M_{u,Rk}}{\gamma_{M1}}}\right)^{\xi} + k_{uv}\frac{M_{v,Ed}}{\frac{M_{v,Rk}}{\gamma_{M1}}} \leq 1 \qquad \textbf{Eq. 3.17}$$

$$\left(\frac{N_{Ed}}{\chi_v \frac{N_{Rk}}{\gamma_{M1}}} + k_{vu}\frac{M_{u,Ed}}{\chi_{LT}\frac{M_{u,Rk}}{\gamma_{M1}}}\right)^{\xi} + k_{vv}\frac{M_{v,Ed}}{\frac{M_{v,Rk}}{\gamma_{M1}}} \leq 1 \qquad \textbf{Eq. 3.18}$$

According to section 3.3.4.2, the exponent is equal to:

$\xi = 1{,}5$ for SBE members

$\xi = 1{,}1$ for SBU members

Figure 3.20 represents the results obtained for the members studied in sections 3.3.4.1 and 3.3.4.2:

- SBE: 2 L70x70x7 with fit bolts;
- SBU: L90x90x9 + L60x60x6 with fit bolts.

One may again observe that the results are very satisfactory and that the interaction equations provide a sufficient and not excessive safety margin. Additionally, the standard deviation is very low and hence it seems possible to determine a partial factor not exceeding 1. The calculation of the partial factor is provided in the next section for all configurations. Nonetheless, Figure 3.20 shows that the design model applied to SBU specimens is slightly less conservative than for SBE specimens. The exponent ξ could be reduced. However, this is not done here as the reliability study summarised in section 3.4 highlights that the proposed interaction equations provide a sufficient reliability.

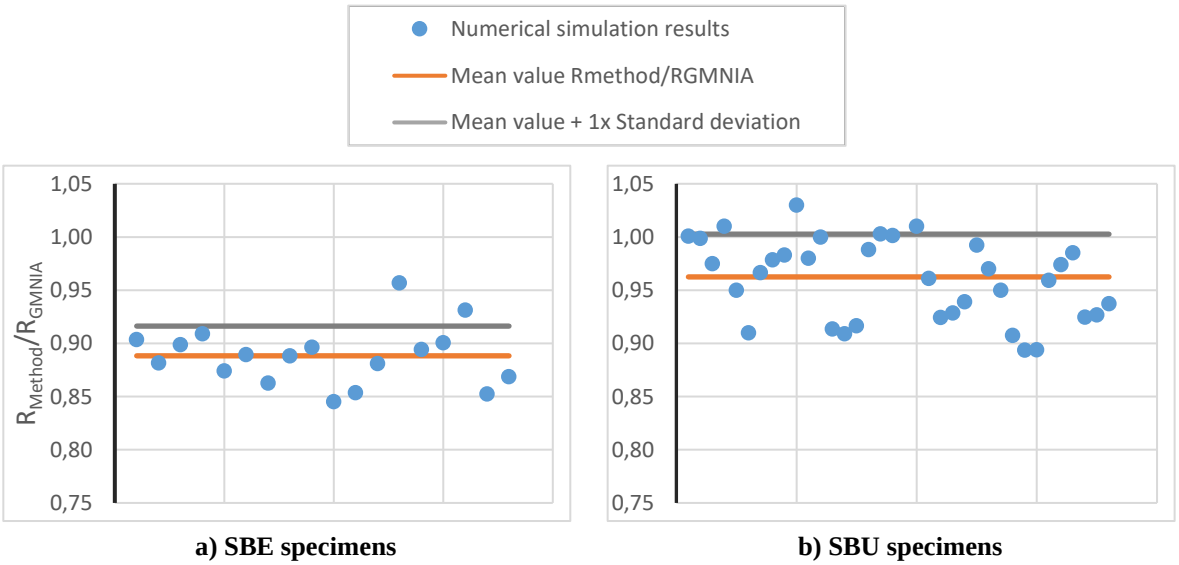

a) SBE specimens **b) SBU specimens**

Figure 3.20: Resistance of SBE and SBU specimens subject to combined axial force and major axis bending

3.4 Reliability and determination of the partial factor

3.4.1 General procedure

Hereafter, the partial factors to be applied to the developed design procedure are determined according to the principles of EN 1990 [13] and the recommendations given in the framework of the RFCS project SAFEBRICTILE [14].

The procedure applied for the determination of the partial factor can be divided into 4 main steps:

- Step 1: Preparation of the input data – Resistance function g_{rt}, reference results r_e and statistical distribution of the basic variables (noted X Figure 3.21);
- Step 2: Evaluation of the precision of the resistance function;
- Step 3: Determination of the sensitivity of the resistance function to variations of the basic variables;
- Step 4: Determination of the design resistance r_d and the partial factor γ_M to be applied to the nominal resistance calculated with the design method.

These steps are illustrated in Figure 3.21. The first step, the resistance function should be determined. This function g_{rt} provides the resistance for a given failure mode (for example flexural buckling) depending on the input variables. In the framework of ANGELHY, the resistance function g_{rt} is the method defined in section 3.2 for the determination of the major axis buckling resistance of BBE specimens and for SBE and SBU specimens, the resistance function corresponds to the interaction equations. The basic variables are all statistical parameters that are considered in the resistance function. For the methods proposed for built-up members in ANGELHY, these parameters are:

- The thickness of the angle sections t;
- The width of the angle sections' legs b;
- The yield stress f_y.

Other parameters are included in the resistance function but, hereafter, they are considered as deterministic, i.e. possessing a mean value equal to the nominal value and a standard deviation equal to 0:

- The radii r_1 and r_2 of the angle section;
- The length L of the member;
- The distribution of the bending moments for SBE and SBU specimens (influencing the critical bending moment and the equivalent uniform moment factor C_{ij});
- The Young's modulus E.

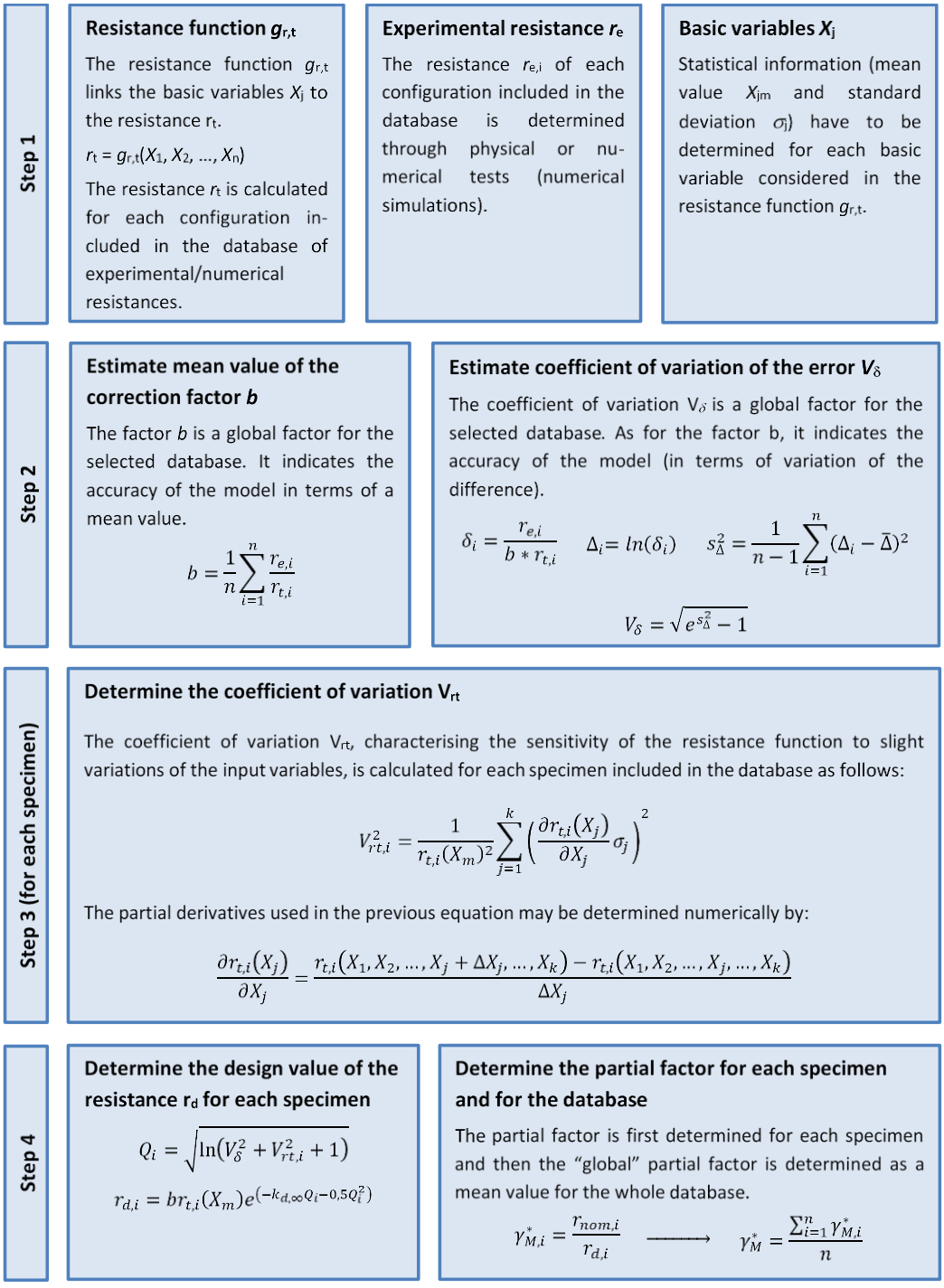

Figure 3.21: Main steps for the determination of the partial factor (Figure from reference [15])

In the second step, the statistical data in terms of precision of the resistance function compared to the reference results is determined. Therefore, the results of the resistance function $r_{t,I}$ are calculated for each configuration contained in the data basis of reference results $r_{e,i}$.

In the third step, the sensitivity of the resistance function to small changes of the input data is determined. As the input data is of stochastic nature, the partial factor is negatively effected, if the sensitivity of the resistance function to variations of input data is high.

Finally, the design value of the resistance is determined based on a given reliability index, characterised by the value of $k_{d,\infty}$ (here 3,04 to respect the reference reliability level of EN 1990), in step 4. The partial factor is the determined as the ratio between the nominal resistance and the design resistance.

Section 3.4.2 presents the statistical data collected in the framework of ANGELHY.

3.4.2 Statistical data

In this section, the partial factor is determined according to Annex D of EN 1090 [13] and the recommendations given in reference [14]. As main input data, it is necessary to possess knowledge on the statistical distribution of the basic variables, i.e. the variables accounted for in the design model. In the framework of ANGELHY, these data have been collected from the measurements performed in the laboratory concerning the material law and the geometric dimensions. Table 3.2 and Table 3.3 present the basic statistical data of the input variables collected in the framework of ANGELHY. These data represent approximatively 100 individual measurements.

Table 3.2: Statistical data material properties

Steel grade	Mean value Ratio Measured yield stress to Nominal yield stress	Standard deviation Ratio Measured yield stress to Nominal yield stress
S235	1,33	4,06%
S355	1,25	6,88%
S460	0,98	7,50%

Table 3.3: Statistical data geometric dimensions

Dimension	Mean value Ratio Measured dimension to Nominal dimension	Standard deviation Ratio Measured dimension to Nominal dimension
Leg width b	1,006	0,8%
Thickness t	0,98	2,6%

Based on the statistical data presented here and the method recalled in section 3.4.1, the partial factor for the design methods is determined in the following sections.

3.4.3 Determination of the partial factor for major axis buckling of BBE specimens

The application of the procedure for the determination of the partial factor is detailed hereafter for the case of back-to-back connected angle sections with fit bolt connections. In section 3.4.4, the partial factors are summarized for all configurations and load cases.

Table 3.4 shows the main results obtained by applying the procedure of section 3.4.1. The notation of the configuration indicates:

- The type of specimen (BBE);
- The connection type (f – fit bolts);
- The angle sections (2 L70x70x7);
- The distance between the packing plates as a multiplier of the minimum radius of gyration (*X*i);
- The number of packing plates (*X*pp).

All members of Table 3.4 are fabricated from S355.

Table 3.4: Determination of the partial factor – main parameters

Configuration	Relative slenderness	Ratio $r_{e,i}/r_{t,i}$	Nominal resistance R_{nom}/R_{pl}	Mean value resistance R_{mean}/R_{pl}	Design resistance R_d/R_{pl}	Partial factor
BBEf_2L70x70x7_15i_2pp	0,277	1,003	0,973	1,189	1,036	0,939
BBEf_2L70x70x7_15i_3pp	0,355	1,021	0,944	1,148	1,002	0,941
BBEf_2L70x70x7_15i_4pp	0,435	1,040	0,912	1,102	0,965	0,945
BBEf_2L70x70x7_15i_6pp	0,599	1,075	0,838	0,992	0,876	0,956
BBEf_2L70x70x7_15i_8pp	0,765	1,078	0,746	0,856	0,766	0,974
BBEf_2L70x70x7_15i_10pp	0,931	1,060	0,641	0,710	0,645	0,994
BBEf_2L70x70x7_15i_13pp	1,181	1,071	0,489	0,519	0,479	1,020
BBEf_2L70x70x7_15i_16pp	1,432	1,057	0,368	0,383	0,355	1,038
BBEf_2L70x70x7_15i_20pp	1,768	1,053	0,260	0,267	0,248	1,051
BBEf_2L70x70x7_30i_2pp	0,553	1,065	0,860	1,025	0,903	0,952
BBEf_2L70x70x7_30i_3pp	0,710	1,081	0,778	0,904	0,805	0,967
BBEf_2L70x70x7_30i_4pp	0,870	1,092	0,680	0,763	0,690	0,987
BBEf_2L70x70x7_30i_6pp	1,198	1,059	0,479	0,509	0,469	1,021
BBEf_2L70x70x7_30i_8pp	1,529	1,041	0,332	0,343	0,318	1,042
BBEf_2L70x70x7_30i_10pp	1,862	1,044	0,238	0,243	0,226	1,054
BBEf_2L70x70x7_30i_13pp	2,363	1,035	0,155	0,157	0,146	1,063
BBEf_2L70x70x7_50i_2pp	0,922	1,105	0,647	0,718	0,652	0,992
BBEf_2L70x70x7_50i_3pp	1,183	1,084	0,488	0,518	0,478	1,020
BBEf_2L70x70x7_50i_4pp	1,451	1,058	0,361	0,375	0,348	1,038
BBEf_2L70x70x7_50i_6pp	1,997	1,039	0,210	0,214	0,199	1,057
	Mean value	1,05			Mean value	1,003

First, Table 3.4 shows that the mean value of the partial factor is equal to 1,0 and consequently the design procedure respects the target reliability level of EN 1990 with the recommended value of the partial factor given in EN 1993-1-1 for stability design checks. Nonetheless, it appears that the partial factor is slightly above 1,0 (up to 1,06) for certain configurations even if the design method yields safe sided results for these configurations (see for example configuration BBEf_2L70x70x7_30i_10pp and BBEf_2L70x70x7_50i_6pp). In order to analyse the results further on, Figure 3.22 represents with the relative slenderness. It appears that the value of the partial factor increases with increasing slenderness. However, as shown in Figure 3.22b this observation cannot be linked to the design method. Indeed, up to a relative slenderness of approximatively 1,0 the ratio $r_{e,i}/r_{t,i}$ increases indicating that the design model becomes more conservative. Consequently, one might suppose that the value of the partial factor decreases. Yet, this is not the case. In fact, the increase of the partial factor is linked to the statistical data of the input variables. For short members, reliability of the design model is positively influenced by the yield strength that exceeds the nominal value by about 25% in average. For longer members, this positive effect vanishes and the member resistance depends to a greater extend on the stiffness of the member that is itself characterised by the second moment of area. As the thickness of angle section is in average 2% less than the nominal value, the reliability is therefore negatively influenced, leading to a higher value of the partial factor for slender members. This observation is also confirmed by observing the results of Table 3.4 again. In fact, the mean value resistance (obtained by applying the design method the mean values of the input data) exceeds highly the nominal value resistance (obtained by applying the design method the nominal values of the input data) for short members, but it becomes nearly identical to the nominal value resistance for slender members.

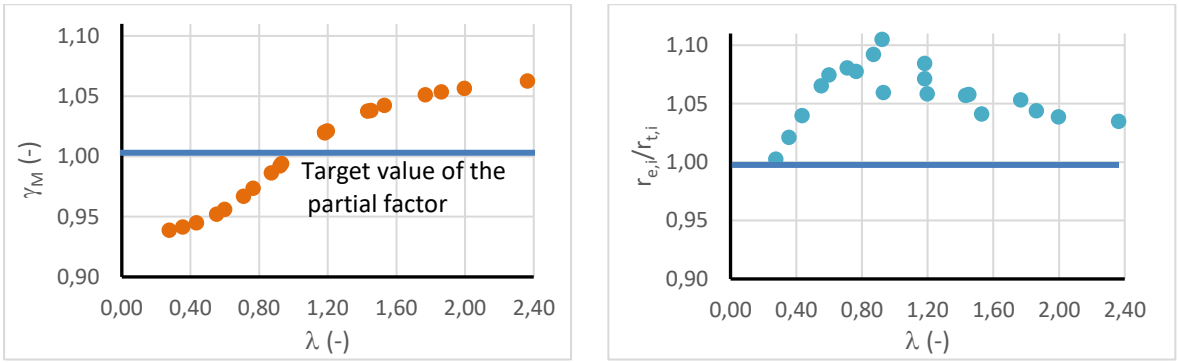

a) Value of the partial factor **b) Ratio between reference result and design model**

Figure 3.22: Evolution of the partial factor and the ratio $r_{e,i}/r_{t,i}$ with the relative slenderness

3.4.4 Synthesis of the obtained partial factors

The partial factor obtained for the different configurations are summarised in Table 3.5. For BBE specimens, the results are detailed depending on the connection type. It appears that the values of the partial factor are very close. For the case of SBE and SBU specimens, the results of the partial factor are therefore given independently from the type of connection. As for BBE specimens, the partial factor is also below 1,0 in case of SBE. For SBU specimens the partial factor is slightly higher than 1,0 but it may still be accepted that a partial factor of 1,0 is used for design. Therefore, it may be concluded that the developed design model may be safely

applied in the field covered by the parametric study. In particular, it is recalled that only compact angle sections are considered. The effect of local buckling on the cross section level has not been included. For more slender sections, the exponent ξ included in the interaction equations should certainly be reduced.

Table 3.5: Summary of partial factors

Configuration	Loading	Partial factor
BBE with fit bolts	Axial force	1,003
BBE with preloaded bolts		1,004
BBE with snug tight bolts		0,984
SBE	Combination of axial force and bending moments	0,955
SBU		1,016

4 References

[1] S. P. Timoshenko and J. M. Gere, *Theory of Elastic Stability*, 2nd ed. Mc Graw Hill International Book Company, 1963.
[2] Engesser, F., 'Die Knickfestigkeit gerader Stäbe', *Zentralbl Bauverwalt.*, vol. 11, pp. 483–486, 1891.
[3] H. H. Snijder, 'Effective second moment of area of uniform built-up members', *Stahlbau*, vol. 87, no. 4, pp. 323–331, Apr. 2018, doi: 10/gg3ww9.
[4] European Committee for Standardization, *Eurocode 3 -Design of steel structures. Part 1-1 : General rules and rules for buildings.* Brussels, 2005.
[5] H. H. Bleich, *Buckling Strength of Metal Structure*. New York, NY: McGraw-Hill Book Company, Inc., 1952.
[6] F. Aslani and S. C. Goel, 'An Analytical Criterion for Buckling Strenght of Built-up Compression Members', *Eng. J.*, vol. 24, no. 4, pp. 159–168, 1991.
[7] 'AISC_Specification_2005-third_print.pdf'. .
[8] A. Sato and C.-M. Uang, 'Modified Slenderness Ratio for Built-up Members', p. 13.
[9] AISC, *ANSI/AISC 360-10 - Specification for Structural Steel Buildings*. Chicago, Ill.: American Institute of Steel Construction, 2010.
[10] ECCS - TC8, *Recommendations For Angles in Lattice Transmission Towers - Publication n°39*. Brussels: ECCS, 1985.
[11] CENELEC, *Overhead electrical lines exceeding AC 1 kV - Part 1: General requirements - Common specifications*. Brussels: Comité Européen de la Normalisation Electrotechnique, 2012.
[12] A. Bureau and P.-L. Chouzenoux, 'Méthode simplifiée pour la vérification de barres comprimées composées de deux cornières assemblées dos-à-dos', *Rev. Constr. Métallique*, no. 4/210, pp. 27–42, 2010.
[13] 'EN 1990: Eurocode - Basis of structural design'. CEN, 2003.
[14] A. Taras, V. Dehan, L. S. da Silva, L. Marques, and T. Tankova, 'SAFEBRICTILE: Standardization of Safety Assessment Procedures across Brittle to Ductile Failure Modes, Grant Agreement Number: RFSR-CT-2013-00023, Deliverable D1.1 – Guideline for the Safety Assessment of Design Rules for Steel Structures in Line with EN 1990',. RFCS, 2016.
[15] A. Beyer, A. Bureau, A. Taras, and A. Toffolon, 'HOLLOSSTAB: Overall-Slenderness Based Direct Design for Strength and Stability of Innovative Hollow Sections, Grant Agreement Number: RFCS-2015-709892, Deliverable D7.2 – Reliability Analysis of the Design Proposals and Determination of Partial Factors'. RFCS, 2019.

List of Figures

List of Tables